Challenge Journal of Structural Mechanics

Research Article

The novelty design method in lightweight structures with low effective elastic modulus

Hojjat Ghahramanzadeh Asl [a,*], Derya Karaman [a]

[a] *Department of Mechanical Engineering, Karadeniz Technical University, 61080 Trabzon, Türkiye*

ABSTRACT

Lightweight structures are of great interest in industrial areas such as automotive, aerospace, and biomedical due to their lightness, and superior mechanical performance. The advantages of lightweight structures are increased with the spread of additive manufacturing and design them in various geometries. Beam-based structures and triply periodic minimal surface structures are currently used to extend these advantages. In this study, it is aimed to create die models of beam-based structures in order to contribute to the geometric diversity for lightweight structures. By designing the die lattice structures of the beam-based structures, the comparison of the mechanical performance of basic lattice and die lattice structures with the same porosity was carried out. For FCC, CFCC, and Octet-Truss lattice structures, basic lattice and die lattice structures are designed on scaffolds in 5x5x5 array with 50%, 60%, 70%, and 80% porosity. Numerical data were obtained for Ti6Al4V with compression tests simulated by applying pressure in the -y direction. According to numerical analyses, the effective elastic modulus decreased due to the increased porosity in both structure models. The CFCC and Octet Truss scaffolds have different force transmission performances. Likewise, this situation is observed in die lattice structures, but the force transmission with the surfaces reveals the difference of the structures. The effective elastic modulus of basic lattice structure with 80% porosity of the Octet Truss structure is approximately twice that of the die lattice structure. Thus, the use of die lattice structures will provide advantages for the design of lightweight structures with low elastic modulus.

ARTICLE INFO

Article history:
Received 6 January 2024
Revised 3 February 2024
Accepted 23 February 2024

Keywords:
Lattice structure
Effective elastic modulus
Finite element analysis
Additive manufacturing

This is an open access article distributed under the CC BY licence.
© 2024 by the Authors.

1. Introduction

With the development of additive manufacturing technologies, lightweight structures are widely used in aerospace, marine, automotive, construction industries, biomedical, etc. in many engineering fields (Ghahramanzadeh Asl et al. 2023; Almalki et al. 2022; Sharma et al. 2022). In addition to the material saving advantage of lightweight structures, their superior performance such as high specific stiffness, strength, and energy absorption capacity are the main reasons for their wide use (Yang et al. 2021). The design and use of lightweight structures are accomplished by two methods: (1) material type variance; and (2) structure design (Sun et al. 2022). It is quite common to use porous structures modeled in various geometries for the design of structures.

Porous structures are formed by material reduction based on mechanical strength in the basic configuration. These reduction techniques are performed with stochastic (foam) or regular (cell architectures) based on topology optimization (Timercan et al. 2021; Feng et al. 2022). Cell architectures are infinitely replicable homogeneous structures in beam or surface-based forms. A wide variety of cell architectures are created with beam or surface forms having various geometrical properties, and thanks to this diversity, the performance requirements of the structures in the systems can be obtained (Wang et al. 2020). Among these structures, beam-based lattice

* *Corresponding author*. Tel.: +90-462-377-3149 ; E-mail address: h.kahramanzade@ktu.edu.tr (H. Ghahramanzadeh Asl)
ISSN: 2149-8024 / DOI: https://doi.org/10.20528/cjsmec.2024.02.002

structures are frequently preferred for porous structures in terms of modeling with simple design methods and accessibility. Beam-based structures are formed by the combination of various numbers of beams at different angles and with nodes. These data are the main parameters that affect the stiffness of the lattice structures as they cause flexing or bending in the beams. These effects of beams have been studied by many researchers. To investigate the design of impact resistant components, Nasrullah et al. (2020) preferred Octet Truss lattice structures to provide a special structural configuration that provides crush deformation. Peng et al. stated that fewer geometric defects of FCC and BCC structures can occur in Simple Cubic (SC), Body Centred Cubic (BCC), Simple Cubic Body Centred Cubic (SC-BCC), and Face Centred Cubic (FCC) lattice structures, which stand out with their energy absorption capabilities. They developed a parametric computational approach and created a numerical framework for estimating fatigue lives (Peng et al. 2020). Gatto et al. (2021) mechanically investigated diamond and rhombic dodecahedron lattice structures for the biomedical industry and experimentally noted that the compression behavior of these lattice structures is quite similar to natural bone. Triply periodic minimal surface structures (TPMS), defined as surface-based structures, are cell architectures that can be extended infinitely in the cartesian space plane. In TPMS structure, two different solid forms (network and sheet solids) are obtained with the same surface equations of the same architecture (Kapfer et al. 2011). Different geometries of lightweight structure, affect both the mechanical and permeability performance of structures. Günther et al. (2022) evaluated the mechanical performance of two lightweight structure geometries in TPMS structures for bone regeneration. As a result of this evaluation, the sheet solid model for cortical bone and the network solid model for trabecular cell architecture were suggested. In the overall assessment of the difference in TPMS structures, sheet solids were noted to have better mechanical properties in relative density compared to network solids (Kapfer et al. 2011; Al-Ketan et al. 2018). These differences are mainly related to the surface properties and wall thickness of the structures. However, these two form states have been expressed only for TPMS structures and no studies have been found in the literature regarding such a situation for beam-based lattices.

Beam-based lattice structures are symmetrical geometries that form repetitive arrays by combining different numbers of beams at different angles and nodes (Du Plessis et al. 2022; Letov et al. 2023). In addition, minimal surface unit cells provide the formation of porous structures where the curvature sum is equal to zero and can be multiplied infinitely in three directions (Fu et al. 2022). According to this information, die lattice models to be obtained from beam-based lattice structures can be considered as a new alternative for lightweight structures modeling, since they have surface properties. Die lattice structures are obtained by forming the basic lattice structures in the opposite direction with reference to their surfaces. As the novelty of this study, both basic models and die models of FCC, CFCC, and Octet Truss architectures are designed with 50%, 60%, 70%, and 80% porosity. To evaluate the mechanical properties difference between the lattice and die structures, the compression tests are simulated by the Finite Element Method and the effective elastic modulus of these lattice structures is determined. Also, the effects of structure type on effective elastic modules are analyzed by ANOVA. In addition, as a result of the equation obtained from OriginLab software, the results for the intermediate values can be predicted with high precision.

2. Material and Method

2.1. Design of lattice structures

In this study, FCC, CFCC, and Octet Truss were chosen for beam-based lattice structures. For each architecture, unit cells for both basic lattice structure and die structure were designed with 50%, 60%, 70%, and 80% porosity. Unit cell models with dimensions of 1 mm x 1 mm x 1 mm were obtained by using SolidWorks software. Die lattice structures were obtained by evacuating the basic lattice structures from the cube with dimensions of 1 mm x 1 mm x 1 mm in the fully filled structure with the cavity command. For this purpose, die lattice structures with 50%, 60%, 70%, and 80% porosity were designed from the basic lattice structures of 20%, 30%, 40%, and 50% porosity of each model (Fig. 1). Structures designed by this method have surface properties such as surface based TPMS structures.

Eq. (1) was used to calculate the porosity of the unit cells:

$$\text{Porosity} = 1 - (\rho_l/\rho_s) \tag{1}$$

In Eq. (1), ρ_l is the density of the lattice structures and ρ_s that of the solid from which it is obtained (Ashby et al. 2006). A priority classification according to the number of beams and nodes in beam-based structures is determined according to Maxwell's stability criterion (Eq. (2)) (Calladine et al. 1978).

$$M = b - 3j + 6 \tag{2}$$

In this criterion b and j terms are the number of beams and the number of nodes, respectively. The schematic representation of the terms in the equation was given in Fig. 2.

By determining the M criterion, the behavior of beam lattice structures under load is classified. Also, if $M<0$, bending in the structures is dominant, and if $M \geqslant 0$, stretching is dominant in the structure (Deshpande et al. 2001). The specified Maxwell criterion will apply to the basic models. Considering the design rules of die lattice, they are modeled on a surface basis, unlike beam structures. Therefore, this criterion cannot be applied to die lattice structures.

2.2. Finite element analysis

Scaffolds were modeled in 5x5x5 array at the x, y, and z direction with unit cells and the labeling of these models was given in Table 1.

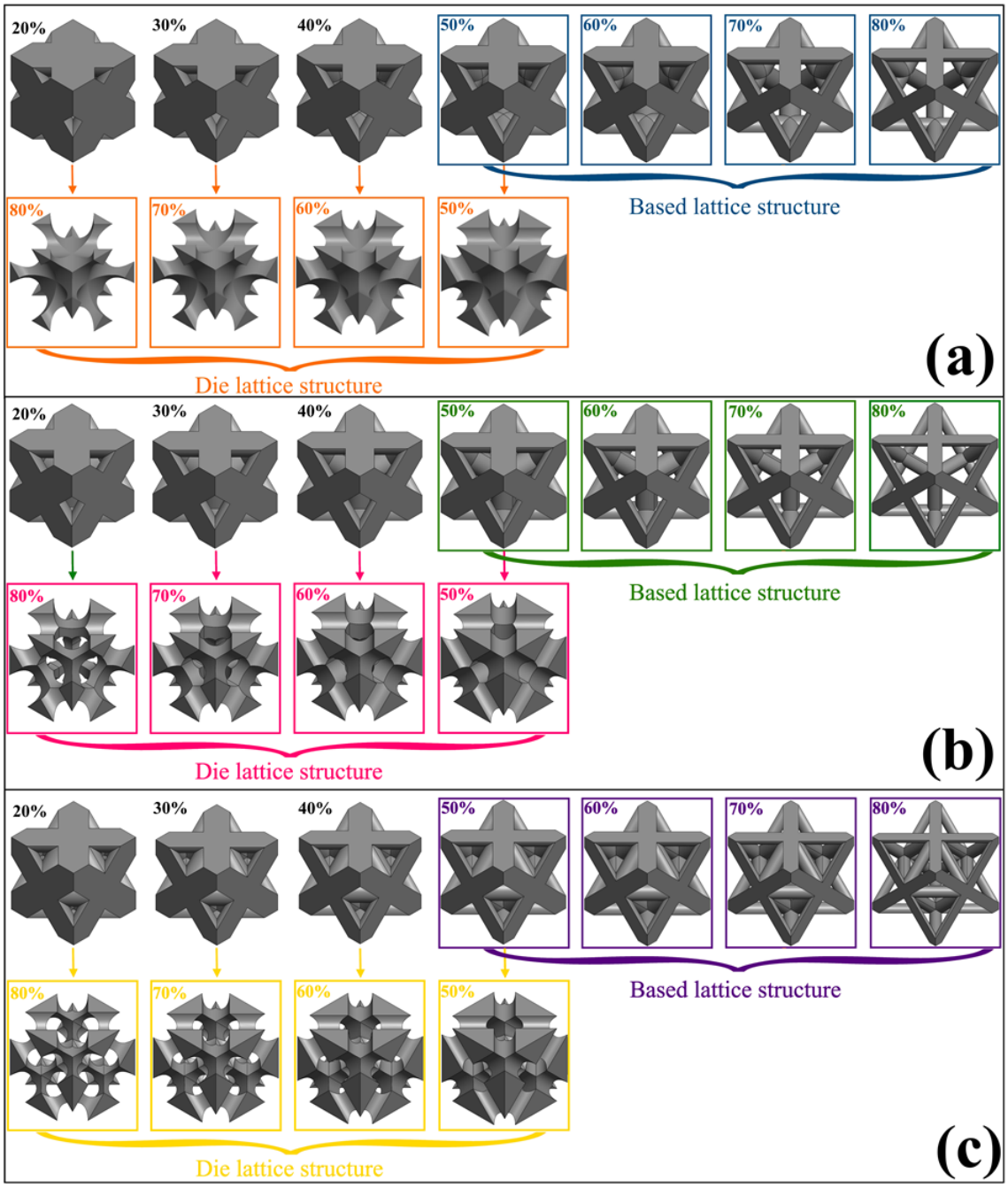

Fig. 1. Unit cells of die lattice structures designed using basic lattice structures: (a) FCC; (b) CFCC; (c) Octet Truss.

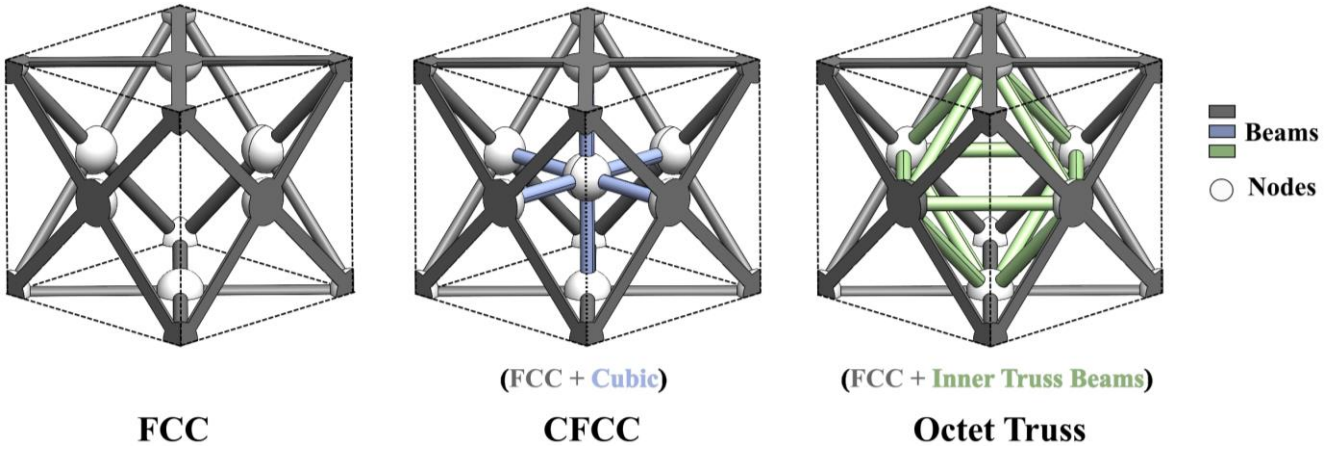

Fig. 2. Beams and nodes of FCC, CFCC, and Octet Truss unit cells.

Table 1. Labeling of scaffold structures.

Unit cell	Type of structure	Porosity			
		50%	60%	70%	80%
FCC	Basic lattice	FCC-50	FCC-60	FCC-70	FCC-80
	Die lattice	FCC_d-50	FCC_d-60	FCC_d-70	FCC_d-80
CFCC	Basic lattice	CFCC-50	CFCC-60	CFCC-70	CFCC-80
	Die lattice	$CFCC_d$-50	$CFCC_d$-60	$CFCC_d$-70	$CFCC_d$-80
Octet Truss	Basic lattice	Octet-50	Octet-60	Octet-70	Octet-80
	Die lattice	$Octet_d$-50	$Octet_d$-60	$Octet_d$-70	$Octet_d$-80

The mechanical performances of the scaffolds were determined according to the effective elastic modulus values. For this determination, compression tests on the scaffolds were simulated. Rigid plates were added to the top and bottom of the scaffold models (Fig. 3a). Plate-mounted scaffolds were transferred to the ANSYS Workbench software, and mesh structures were created. Especially due to the complex geometry of the latticed structure, the mesh element selection was performed as program controlled. The mesh grit of the structure was shown in Fig. 3b.

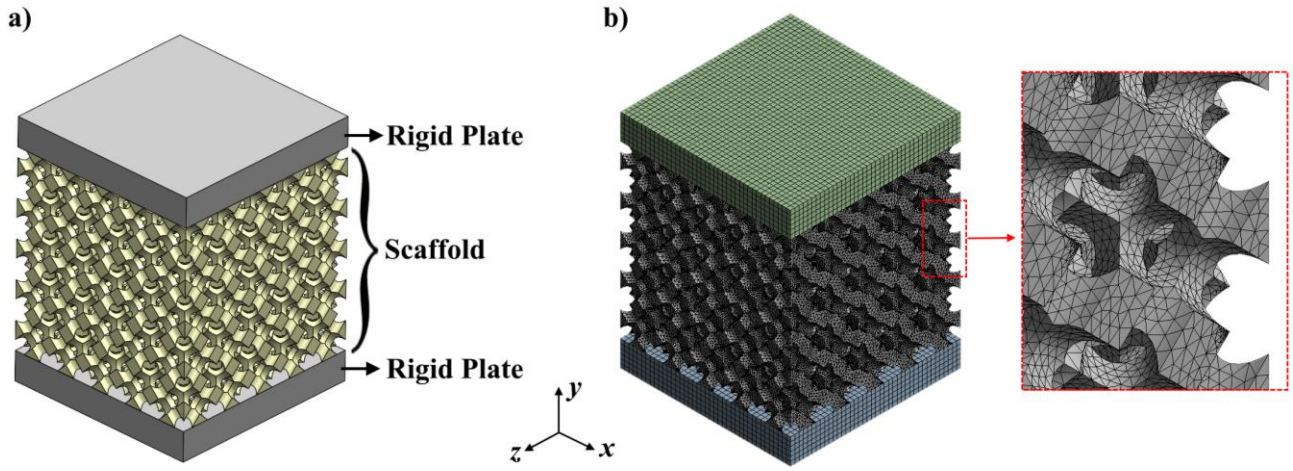

Fig. 3. Compression test models of scaffold; and b) sample mesh structure consisting of tetrahedral elements.

In order to determine the optimum mesh structure, mesh convergence tests with tetrahedral elements were applied and mesh structures with a number of approximately 1.5 million elements were accepted for analysis. The finite element analyses were defined as fixed plane for the bottom plate for the boundary conditions, fixed in the *x* and *z* directions for the top plate, and free in the *y* direction. The scaffold contact surfaces of both plates were defined as bonded (Karaman et al. 2022). As the analysis conditions, a compression pressure of 1 MPa was applied in the *-y* direction. Ti6Al4V alloy was selected as the material where the elastic modulus was 110 GPa and the Poisson ratio was 0.33 as material properties (Xu et al. 2019). As a result of these analyses, the effective elastic modulus (E_{eff}) values of each scaffold were calculated according to Hooke's law. In Hooke's law:

$$\sigma = E \times \varepsilon \qquad \varepsilon = \frac{\Delta L}{L_0} \qquad E_{eff} = \left(\frac{\sigma}{\varepsilon}\right) = \frac{(\sigma \times L_0)}{\Delta L} \qquad (3)$$

In Eq. (3), σ, L_0, and ΔL are the applied pressure (MPa), the initial length of the model (mm), and directional deformation (mm), respectively.

Additionally, a statistical analysis was performed to determine the parameters using the effective elastic modulus data of the scaffolds. One-way analysis of variance was used to investigate statistically significant differences (ANOVA). A p-value less than 0.05 was considered to indicate a statistically significant difference. Furthermore, the curve fitting technique was used to determine the closest match via analyzing the correlation between the dependent and independent variables and constructing a mathematical function, either linear or nonlinear, which includes the curve according to the data points in the collection. The input parameters for this investigation were (*x, y, z*). The data obtained from each scaffold model were analyzed using OriginLab software for evaluating the architecture and porosity of the unit cell. Thus, the effects of design method on effective elastic modules are more clearly understood. In addition, as a result of the equation obtained, the results for the intermediate values can be predicted with high precision.

3. Results and Discussion

The maximum von-Mises stress values that occur in scaffold structures because of compression tests are given in Table 2. According to von-Mises stress values, all scaffolds do not exceed the yield strength in compression of the Ti alloy (970 MPa). Maximum stress values are realized in 80% porous scaffolds in the same architectures. However, the maximum von-Mises stress of the scaffolds gradually increases with increasing porosity.

Table 2. Maximum von-Mises stress values of scaffold structures.

Porosity	von-Mises stress (MPa)					
	FCC	FCC_d	CFCC	$CFCC_d$	Octet	$Octet_d$
50%	18.43	19.31	22.40	15.13	26.97	13.49
60%	26.32	29.37	27.15	26.34	38.13	21.42
70%	41.39	47.16	35.95	44.57	60.12	45.24
80%	74.30	104.64	59.32	89.95	96.70	201.23

The stress distributions occurred in each lattice structure are shown in Fig. 4. The stress distribution of the scaffolds is relatively uniform in von-Mises stress counters. This represents the excellent stress transmission properties of the lattice structures (Nasrullah et al. 2020). When the basic lattice models are evaluated as quantitative amounts, the order of stress values is Octet>CFCC>FCC for 50% and 60% porosity. For 70% and 80% porosity, it is Octet>FCC>CFCC. The occurrence of higher von Mises stress values in the Octet Truss lattice structure compared to both lattice structures is related to the number of beams (Viswanath et al. 2022). It has more beams while having the same number of nodes as FCC. This increases the stress by causing the load density at the joint intersection point in the structure. The variability between FCC and CFCC structures with increasing porosity can be expressed in a similar method. The beams intersecting at the node point in the body center of CFCC structures affect the mechanical behavior of the structure (Zheng et al. 2019). CFCC structures do not differ much from FCC up to 60% porosity. However, with the decrease of the cross-sectional area after 70% porosity, high stresses occur in FCC structures due to structural refining (Zheng et al. 2019). A classical quantitative sort cannot be established for die lattice structures. There are different quantitative sorts within each porosity group. This is affected by the variability of the number of beams and the location of the node points that forming the cavity in the die lattice structures. FCC die lattice structures have a higher tensile value compared to other structures up to 70% porosity. At 80% porosity, Octetd scaffold has the highest stress (201.23 MPa). It is known in the literature that the yielding behavior occurs at 45° during loading in structures (Xu et al. 2019). The cavities created at 45° in the die lattice structures are the main cause of the high stresses. According to the maximum von-Mises stresses, the FCC and CFCC basic lattice structures have lower stress values than the die lattice structures. For Octet Truss, this is the opposite, except for 80% porosity. Octet die lattice structures have lower stress values compared to basic lattice structures. This is all about the angle of cavities formation and the variability in the cross-sectional area of the structure.

The directional deformation values within the elastic limits according to the compression analyses are given in Table 3. For all structures, the directional deformation value increases with the increase in porosity.

In Fig. 5, the visuals of the directional deformations in the structures are given. For all structures, the directional deformation value increases with the increase in porosity. At 50% porosity, the values of the basic lattice structures and the die lattice structures are relatively close to each other. However, with increasing porosity, this situation disappears. With the increase in porosity, the solid volume in the structures decreases and the cross-sectional area decreases (Pham et al. 2020). These refining in the structures reduce the resistance to the force which applies from the y direction. Thus, the directional deformation values increase.

Table 3. Directional deformation values on the scaffolds.

Porosity	Directional deformation (mm) (*y* axis)					
	FCC	FCC_d	CFCC	$CFCC_d$	Octet	$Octet_d$
50%	0.00021012	0.00020916	0.00021680	0.00021223	0.00025220	0.00027175
60%	0.00032741	0.00034049	0.00031772	0.00033906	0.00038795	0.00047018
70%	0.00055005	0.00064242	0.00049198	0.00061829	0.00063133	0.00094640
80%	0.00104240	0.00177290	0.00085139	0.00147470	0.00114580	0.00288850

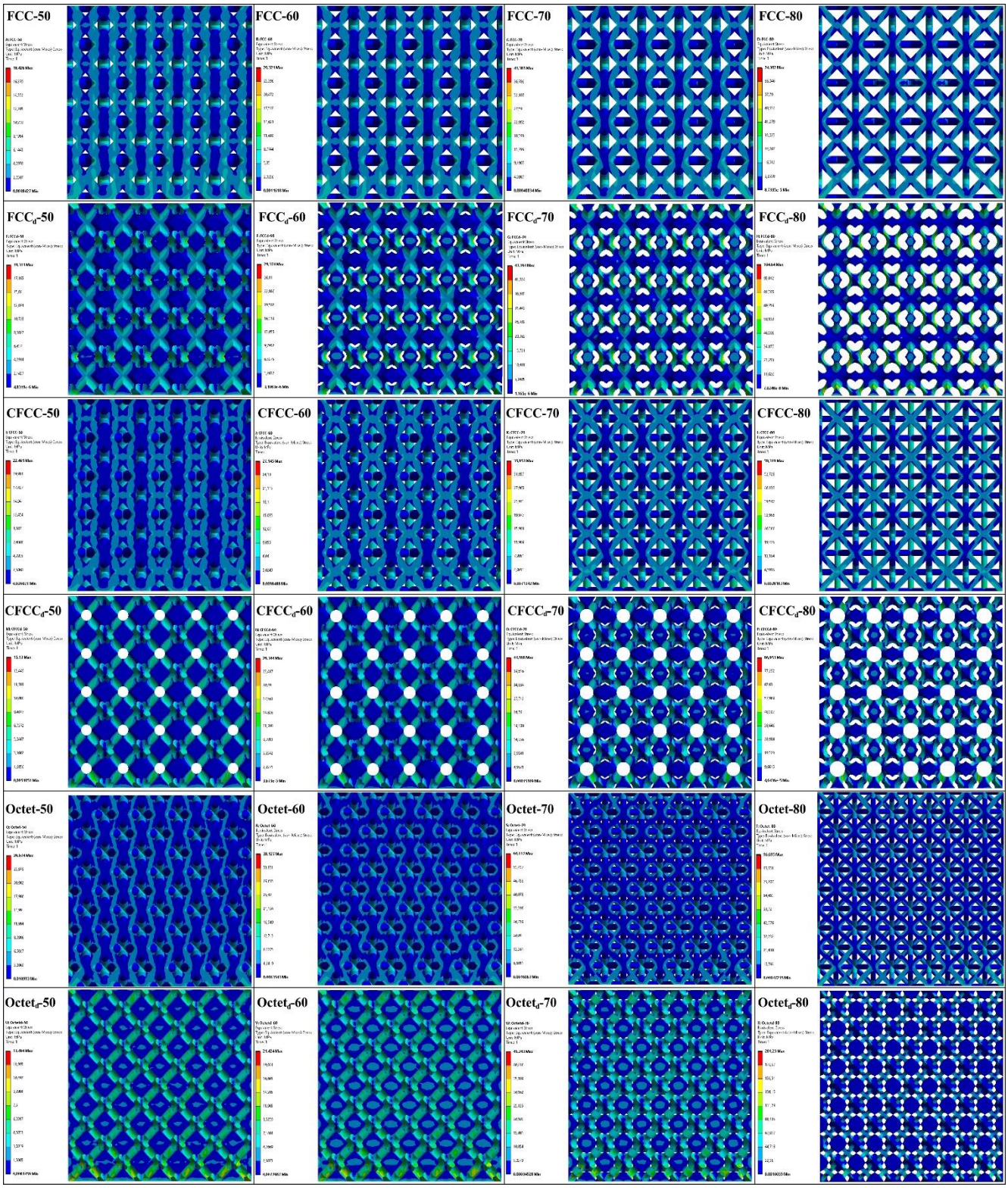

Fig. 4. The distributions of von-Mises stresses occurred in the basic lattice structures and the die lattice structures.

According to the deformation values given in Table 3, the effective elastic modulus values of the scaffolds are calculated according to Hooke's law. Comparison of effective elastic modules of scaffold structures with each other is shown in Fig. 6. In the general impression, the effective elastic modulus value decreases with increasing porosity in the three lattice types. In addition, the die lattice structures of a lattice type, have lower effective elastic modulus values than the basic lattice structures. In FCC and CFCC lattice structures with 50% porosity, basic and die lattice structures are formed at approximately the same values. This situation is not observed in the Octet Truss lattices. Since the directional deformation value in the Octetd-50 model is higher, it has a lower effective elastic modulus compared to the Octet-50.

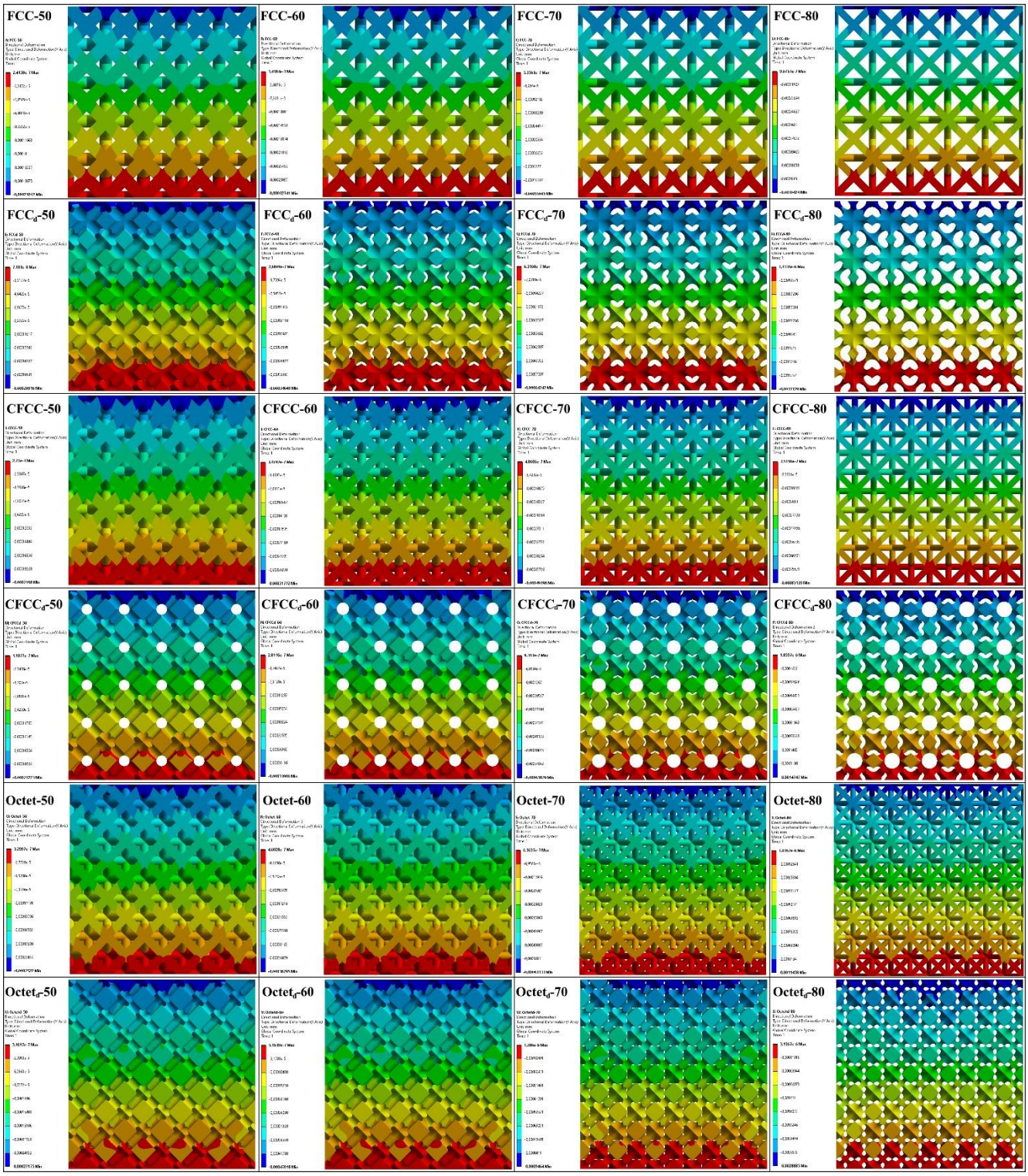

Fig. 5. The distributions of directional deformation (*y*-axis) occurred in the basic lattice structures and the die lattice structures.

With the increase of porosity, the elastic modulus between the basic lattice structure and the die lattice structure increases at different rates in the same lattice type. For example, there is a 3.8% difference between FCC-60 and FCCd-60 structures, 14.4% between FCC-70 and FCCd-70 structures, and 41.2% between FCC-80 and FCCd-80 structures. While there is a 6.29% difference between CFCC-60 and CFCCd-60 structures in CFCC lattice structures, there is 20.4% difference between CFCC-70 and CFCCd-70 structures, and 42.2% difference between FCC-80 and FCCd-80 structures. In Octet Truss lattice structures, these difference values occur significantly at 50% porosity. There is a difference of 7.2% between Octet-50 and Octetd-50, 17.5% between Octet-60 and Octetd-60, 33.3% between Octet-70 and Octetd-70, and 60.3% between Octet-80 and Octetd-80. The reason for the increase in the differences is the increase in the directional deformation values.

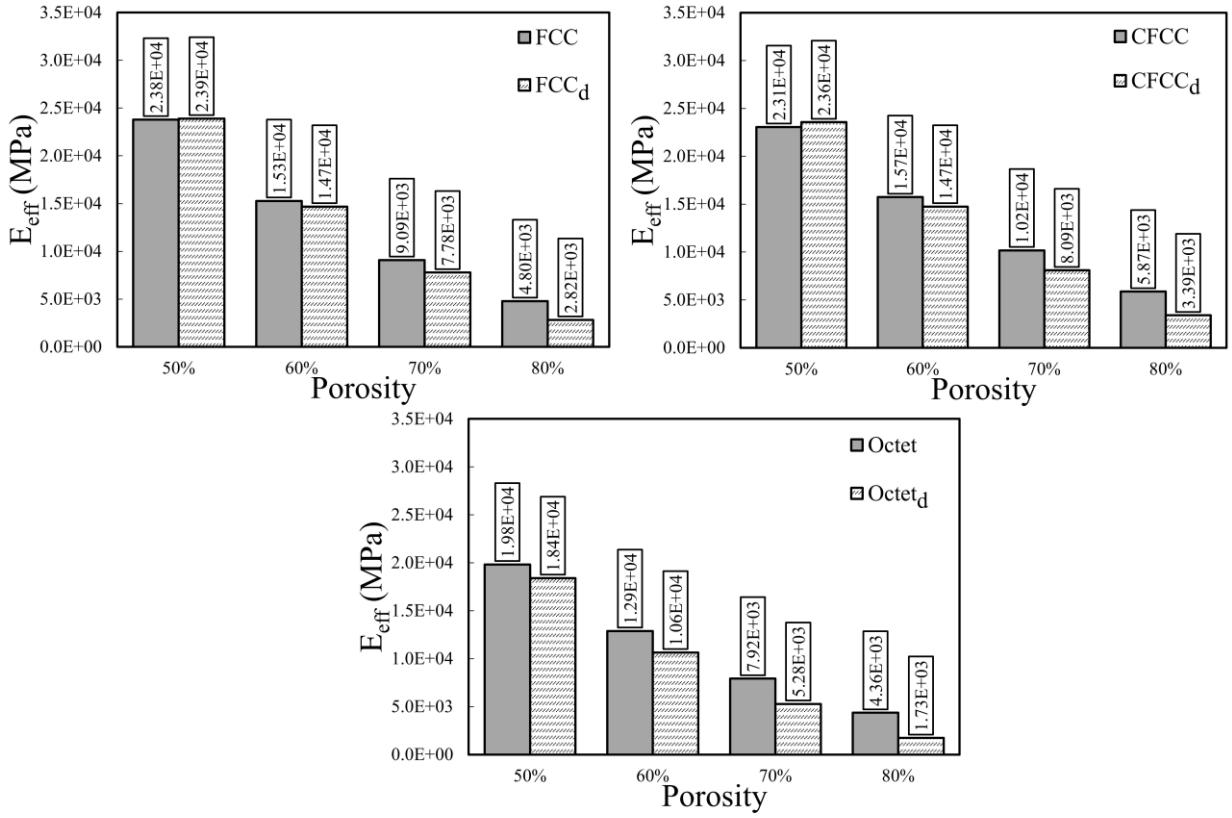

Fig. 6. Effective elastic modulus plot of basic lattice structures and die lattice structures of FCC, CFCC, and Octet Truss.

Octet Truss lattice structures have lower elastic modulus values than other lattice structures. This situation can be associated with Maxwell values (Table 4).

Table 4. Maxwell's criteria for beam-based unit cells.

	FCC	CFCC	Octet Truss
Maxwell's number	-12	-9	0

CFCC and Octet Truss lattices are constructed based on the FCC lattice structure by adding different numbers of beams and nodes (Fig. 2). CFCC lattice structure has 1 more number of nodes and 6 additional beams, unlike FCC. In Octet Truss structures, the nodes are the same as the FCC, but the additional 8 beams form a connection between the surface centers. CFCC structures show more strength in loadings from the y direction. The main reason why CFCC lattice structures show relatively higher strength compared to FCC is the nodes located in the center of the body. Refai et al. (2020) reported the effective elastic properties of 17 different beam-based lattices for Titanium material. According to the outputs of their studies, the CFCC model has higher effective elasticity than both FCC and Octet Truss structures of the same porosity. It is advantageous for these structures that the node, which appears as the intersection point of in the body center, has a higher load-bearing potential. In other words, while tension occurs in the beams cross at the center of the volume, it is seen that stronger structures will be obtained by the formation of compression in the outer beams (Park et al. 2022). Octet Truss structures have the lowest strength among these three structures. Although it has the same node as the FCC lattice structure, the increase in beams joining at these nodes causes this low. The vertical load on the lattice structure is covered by 8 beams that converge at a node, and the nodal points are displaced in all three directions. This causes the bending of beams in Octet Truss structures to occur at a higher rate compared to other lattice structures.

Quantitative ordering obtained in the basic lattice structures in terms of strength is valid for die lattice structures. In other words, CFCCd structures have higher effective elastic modulus than FCCd and Octetd. Verma et al. (2022), who investigated the mechanical properties of the contact between metal and polymer, created resin models with the die method. According to numerical analysis, they noted that CFCC die structures have higher tensile strength than Kelvin structures among the structures they investigated. CFCCd has higher strength compared to other lattice structures in the same porosity, while Octetd has the lowest strength. Since there is no beam in these structures, surface behavior is in the foreground. Die lattice structures provide their continuity with surfaces such as minimal surface structures. However, instead of the surface equations in TPMS structures, it can be defined as the beam surfaces forming the cavity. As mentioned in the literature, lattice structures (especially TPMS) are frequently preferred in various industrial areas such as biomedical and heat transfer due to their surface area properties (Dixit et al. 2022). Tang et al. (2023) performed numerical and experimental analyses using TPMS unit cells (Diamond, Gyroid, and I-WP) to improve the heat transfer process and examine

the performance effects. It was stated that the results differ according to the surface geometry and surface area, and they stated that the best result was obtained from the I-WP unit cell. Al-Ketan and Abu Al-Rub (2021), who simplifies the creation of two different unit cells in TPMS structures with the same surface equations, report that the surface areas change depending on the cell architecture. Expressing this difference for use in the biomedical field, Günther et al. (2022) numerically considered that the network and sheet solids of TPMS structures can provide alternatives for different bone tissues. The die lattice structures created in this study also have a minimal surface geometry similar to TPMS structures. Due to these properties, the load bearing and mechanical strength properties vary according to the surface geometry. Surface geometries will change according to the angles of various beam numbers in beam-based structures.

As a result of statistical analyses, S/N ratio charts are given in Fig. 7 for the effect levels of parameters on the mechanical performance of scaffold structures. The signal value (S) in this sentence refers to the value that has to be measured, while the noise value (N) represents the level at which contaminants affect the measured value. The graphs of the obtained signal-to-noise ratios show the extent of impact of each variable parameter used in the investigation. ANOVA analysis was used to ascertain the significant levels of variable factors that impact the mechanical characteristics of the constructions, in addition to the S/N ratio. The Minitab program was used to carry out this research.

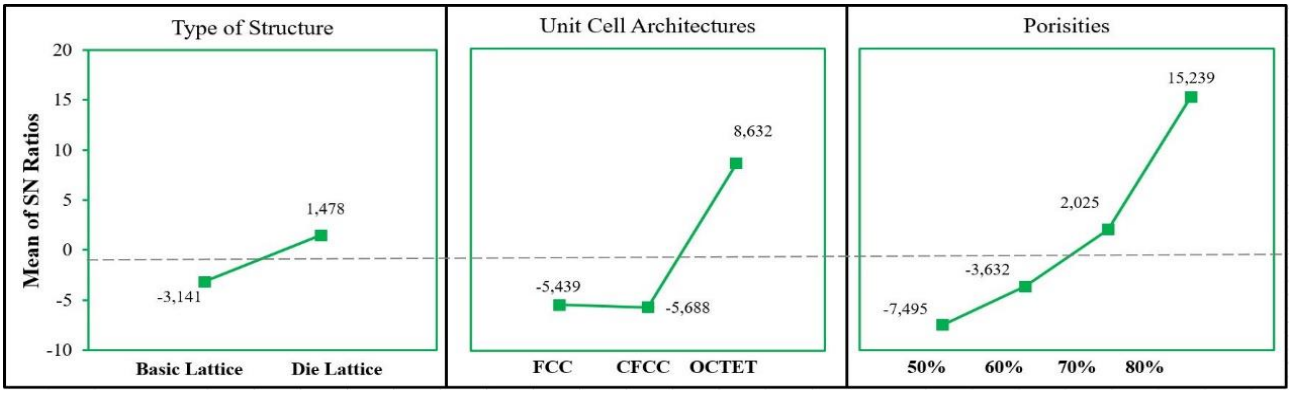

Fig. 7. Influence of the evaluated parameters on the effective elastic modulus.

The residual error of 0.08% is the foundation for these graphics. The charts show that porosity, unit cell architecture, and type of structure have an impact on the effective elastic modulus of the scaffold, accordingly. In this evaluation, porosity is considered the most important parameter at a rate of 54.55%. The effect of unit cell architecture is 34.36%. Type of structures are 11.01% effect on the mechanical performance of the scaffolds. As can be seen from this analysis, the effect of the structure type is significant. With the use of this structure type, scaffold structures with a lower elastic modulus can be obtained. On the other hand, Effective elastic modulus values are transferred to OriginLab software to establish the relationship between results achieved. For each type of structure, equations are obtained using the curve fitting method in OriginLab software according to all unit cell architecture and porosities. Considering the scaffold structure type first, if the "x" value is unit cell architecture and the "y" value is taken as porosity rates (%), the following equations and R squared values for each structure type are seen in Table 5. These curve fitting observations are shown graphically in Fig. 8.

Table 5. Curve fitting analysis results in terms of scaffold structure type.

Cure fitting equation	Structure type	Constants values	R-square
$f(x,y,z) = a_0 + a.x + b.y + c.x^2 + d.y^2 + e.x.y$	Basic lattice	$a_0 = 91063 \pm 1476$ $a = 1013 \pm 121$ $b = -1841 \pm 43$ $c = -1471 \pm 58$ $d = 8.85 \pm 0.35$ $e = 59.55 \pm 3.10$	0.999
	Die lattice	$a_0 = 103322 \pm 1417$ $a = 706 \pm 87$ $b = -2165 \pm 51$ $c = -1793 \pm 110$ $d = 10.57 \pm 0.79$ $e = 74.15 \pm 7.88$	0.998

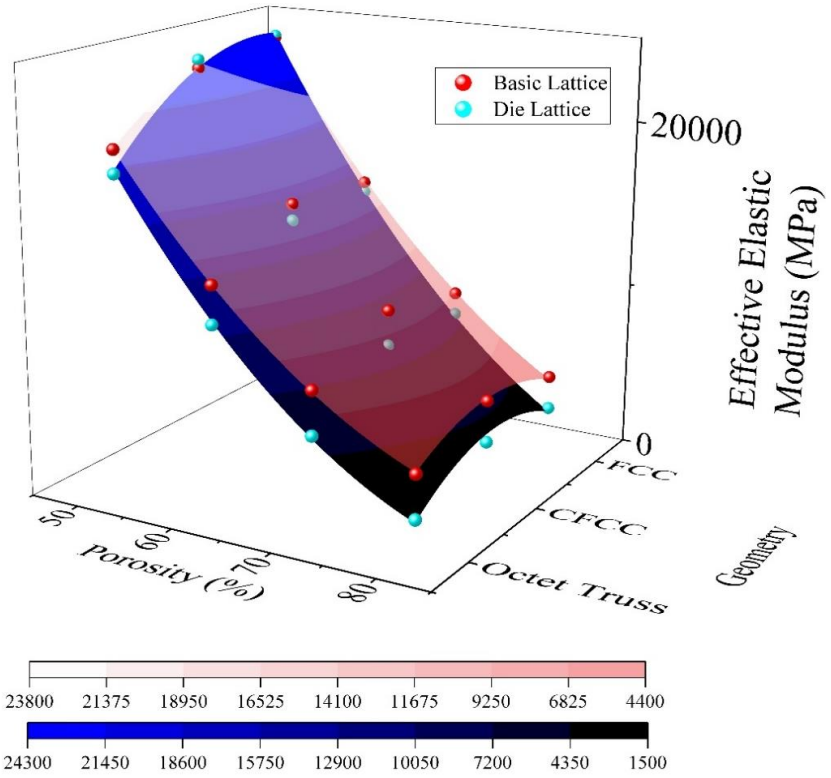

Fig. 8. The graphics of curve fitting results for each structure type.

By using the equations given in Table 5, it will be possible to obtain how much effective elastic modulus of scaffolds will have with inserting the elastic modulus value of the unit cell architecture and the porosity desired to be produced into the equations.

4. Conclusions

In this study, the usability of die structures based on beam-based structures for lightweight structures was investigated. The basic lattice structures and die lattice structures of FCC, CFCC, and Octet Truss unit cells were modeled at 50%, 60%, 70%, and 80% porosity. Mechanical strength properties of a total of 24 lattice structures were analyzed numerically. The directional deformation values in lattice structures with the same architecture increased as the porosity increased in both the basic lattice structure and the die lattice structures. These increases caused a decrease in the effective elastic modules for both structures as the porosity increased. Both the basic lattice structure and the die lattice structure of the CFCC architecture show higher mechanical strength compared to other architectures. In addition, die lattice structures with the same porosity in architecture have lower effective elastic modules. As a result of the ANOVA analysis, it was seen that the structure type had an effect of ~11%. The main reason for this is that surface connections come in effectively instead of beams for load transmission. The study provides a reference for innovating design configurations of lattice structures by modeling lightweight structures with low elastic modulus. The polynomial equations, which represent second-order curves, were classified into three groups based on the curve fitting approach used to the data received from finite element analysis. The coefficient of determination (R-square) for these equations exceeded 0.99. The formulae provided allow for the calculation of the effective elastic modulus without any restrictions, by using two established constant values related to the relevant fields. The calculated correlations for the curve equation demonstrated adequate accuracy for the engineering field. Because of their use, these curve equations provide an abundance of options for the geometric and mechanical characteristics of the structure, thus providing an invaluable resource for production planning in an efficient way.

Acknowledgements

None declared.

Funding

The authors received no financial support for the research, authorship, and/or publication of this manuscript.

Conflict of Interest

The authors declared no potential conflicts of interest with respect to the research, authorship, and/or publication of this manuscript.

Author Contributions

All of the authors made substantial contributions to conception and design, or acquisition of data, or analysis and interpretation of data; were involved in drafting the manuscript or revising it critically for important intellectual content; and gave final approval of the version to be published.

Data Availability

The datasets created and/or analyzed during the current study are not publicly available, but are available from the corresponding author upon reasonable request.

REFERENCES

Al-Ketan O, Rowshan R, Al-Rub RKA (2018). Topology-mechanical property relationship of 3D printed strut, skeletal, and sheet based periodic metallic cellular materials. *Additive Manufacturing*, 19, 167-183.

Al-Ketan O, Abu Al-Rub RK (2021). MSLattice: A free software for generating uniform and graded lattices based on triply periodic minimal surfaces. *Material Design and Processing Communications*, 3(6), e205.

Almalki A, Downing D, Lozanovski B, Tino R, Du Plessis A, Qian M Brandt M, Leary M (2022). A digital-twin methodology for the non-destructive certification of lattice structures. *JOM*, 74(4), 1784-1797.

Ashby MF (2006). The properties of foams and lattices. *Philosophical Transactions of the Royal Society A: Mathematical, Physical and Engineering Sciences*, 364(1838), 15-30.

Calladine CR (1978). Buckminster Fuller's "tensegrity" structures and Clerk Maxwell's rules for the construction of stiff frames. *International Journal of Solids and Structures*, 14(2), 161-172.

Deshpande VS, Ashby MF, Fleck NA (2001). Foam topology: bending versus stretching dominated architectures. *Acta Materialia*, 49(6), 1035-1040.

Dixit T, Al-Hajri E, Paul MC, Nithiarasu P, Kumar S (2022). High performance, microarchitected, compact heat exchanger enabled by 3D printing. *Applied Thermal Engineering*, 210, 118339.

Du Plessis A, Razavi SMJ, Benedetti M, Murchio S, Leary M, Watson M, Bhate D, Berto F (2022). Properties and applications of additively manufactured metallic cellular materials: A review. *Progress in Materials Science*, 125, 100918.

Feng Y, Huang T, Gong Y, Jia P (2022). Stiffness optimization design for TPMS architected cellular materials. *Materials & Design*, 222, 111078.

Fu H, Kaewunruen S (2022). Experimental and DEM investigation of axially-loaded behaviours of IWP-based structures. *International Journal of Mechanical Sciences*, 235, 107738.

Gatto ML, Groppo R, Bloise N, Fassina L, Visai L, Galati W, Iuliano L, Mengucci P (2021). Topological, mechanical and biological properties of Ti6Al4V scaffolds for bone tissue regeneration fabricated with reused powders via electron beam melting. *Materials*, 14(1), 224.

Ghahramanzadeh Asl H, Altıntaş Kahriman E, Karaman D (2023). Numerical investigation of the effective mechanical properties of Octet Truss lattice structures with different strut geometry. *Challenge Journal of Structural Mechanics*, 9(4), 133-144.

Günther F, Wagner M, Pilz S, Gebert A, Zimmermann M (2022). Design procedure for triply periodic minimal surface based biomimetic scaffolds. *Journal of the Mechanical Behavior of Biomedical Materials*, 126, 104871.

Kapfer SC, Hyde ST, Mecke K, Arns CH, Schröder-Turk GE (2011). Minimal surface scaffold designs for tissue engineering. *Biomaterials*, 32(29), 6875-6882.

Karaman D, Ghahramanzadeh Asl H, Altıntaş Kahriman E (2022). Estimation and comparison of effective elastic modulus of different scaffolds using curve fitting method for additive manufacturing field. *Arabian Journal for Science and Engineering*, 47, 15973–15987.

Letov N, Fiona Zhao Y (2023). Beam-based lattice topology transition with function representation. *Journal of Mechanical Design*, 145(1), 011704.

Nasrullah AIH, Santosa SP, Dirgantara T (2020). Design and optimization of crashworthy components based on lattice structure configuration. *Structures*, 26, 969-981.

Park SJ, Lee JH, Yang J, Heogh W, Kang D, Yeon SM, Kim SH, Hong S, Son Y, Park J (2022). Lightweight injection mold using additively manufactured Ti-6Al-4V lattice structures. *Journal of Manufacturing Processes*, 79, 759-766.

Peng C, Tran P, Nguyen-Xuan H, Ferreira A (2020). Mechanical performance and fatigue life prediction of lattice structures: Parametric computational approach. *Composite Structures*, 235, 111821.

Pham A, Kelly C, Gall K (2020). Free boundary effects and representative volume elements in 3D printed Ti–6Al–4V gyroid structures. *Journal of Materials Research*, 35(19), 2547-2555.

Refai K, Montemurro M, Brugger C, Saintier N (2020). Determination of the effective elastic properties of titanium lattice structures. *Mechanics of Advanced Materials and Structures*, 27(23), 1966-1982.

Sharma D, Hiremath SS, Kenchappa NB (2022). Bio-inspired Ti-6Al-4V mechanical metamaterials fabricated using selective laser melting process. *Materials Today Communications*, 33, 104631.

Sun G, Chen D, Zhu G, Li Q (2022). Lightweight hybrid materials and structures for energy absorption: A state-of-the-art review and outlook. *Thin-Walled Structures*, 172, 108760.

Tang W, Zhou H, Zeng Y, Jiang C, Yang P, Li Q, Fu J, Huang Y, Zhao Y (2023). Analysis on the convective heat transfer process and performance evaluation of Triply Periodic Minimal Surface (TPMS) based on Diamond, Gyroid and Iwp. *International Journal of Heat and Mass Transfer*, 201, 123642.

Timercan A, Sheremetyev V, Brailovski V (2021). Mechanical properties and fluid permeability of gyroid and diamond lattice structures for intervertebral devices: functional requirements and comparative analysis. *Science and Technology of Advanced Materials*, 22(1), 285-300.

Verma S, Yang CK, Lin CH, Jeng JY (2022). Additive manufacturing of lattice structures for high strength mechanical interlocking of metal and resin during injection molding. *Additive Manufacturing*, 49, 102463.

Viswanath A, Khan KA, Barsoum I (2022). Design of novel isosurface strut-based lattice structures: Effective stiffness, strength, anisotropy and fatigue properties. *Materials & Design*, 224, 111293.

Wang C, Gu X, Zhu J, Zhou H, Li S, Zhang W (2020). Concurrent design of hierarchical structures with three-dimensional parameterized lattice microstructures for additive manufacturing. *Structural and Multidisciplinary Optimization*, 61, 869-894.

Xu Y, Zhang D, Hu S, Chen R, Gu Y, Kong X, Tao J, Jiang Y (2019). Mechanical properties tailoring of topology optimized and selective laser melting fabricated Ti6Al4V lattice structure. *Journal of the Mechanical Behavior of Biomedical Materials*, 99, 225-239.

Yang JS, Chen SY, Li S, Pang YZ, Schidt R, Schröder KU, Qu J, Wu LZ (2021). Dynamic responses of hybrid lightweight composite sandwich panels with aluminum pyramidal truss cores. *Journal of Sandwich Structures & Materials*, 23(6), 2176-2195.

Zheng HD, Liu LL, Deng CL, Shi Z, Ning C (2019). Mechanical properties of AM Ti6Al4V porous scaffolds with various cell structures. *Rare Metals*, 38, 561-570.